

See discussions, stats, and author profiles for this publication at: <https://www.researchgate.net/publication/221111151>

# ORB: an efficient alternative to SIFT or SURF

Conference Paper in Proceedings / IEEE International Conference on Computer Vision. IEEE International Conference on Computer Vision · November 2011

DOI: 10.1109/ICCV.2011.6126544 · Source: DBLP

---

CITATIONS

6,121

---

READS

21,641

4 authors, including:



Ethan Rublee

Self

3 PUBLICATIONS 6,173 CITATIONS

SEE PROFILE



Gary Bradski

Industrial Perception

51 PUBLICATIONS 17,437 CITATIONS

SEE PROFILE

# ORB: an efficient alternative to SIFT or SURF

Ethan Rublee

Vincent Rabaud

Kurt Konolige

Gary Bradski

Willow Garage, Menlo Park, California

{erublee}{vrabaud}{konolige}{bradski}@willowgarage.com

## Abstract

*Feature matching is at the base of many computer vision problems, such as object recognition or structure from motion. Current methods rely on costly descriptors for detection and matching. In this paper, we propose a very fast binary descriptor based on BRIEF, called ORB, which is rotation invariant and resistant to noise. We demonstrate through experiments how ORB is at two orders of magnitude faster than SIFT, while performing as well in many situations. The efficiency is tested on several real-world applications, including object detection and patch-tracking on a smart phone.*

## 1. Introduction

The SIFT keypoint detector and descriptor [17], although over a decade old, have proven remarkably successful in a number of applications using visual features, including object recognition [17], image stitching [28], visual mapping [25], etc. However, it imposes a large computational burden, especially for real-time systems such as visual odometry, or for low-power devices such as cellphones. This has led to an intensive search for replacements with lower computation cost; arguably the best of these is SURF [2]. There has also been research aimed at speeding up the computation of SIFT, most notably with GPU devices [26].

In this paper, we propose a computationally-efficient replacement to SIFT that has similar matching performance, is less affected by image noise, and is capable of being used for real-time performance. Our main motivation is to enhance many common image-matching applications, e.g., to enable low-power devices without GPU acceleration to perform panorama stitching and patch tracking, and to reduce the time for feature-based object detection on standard PCs. Our descriptor performs as well as SIFT on these tasks (and better than SURF), while being almost two orders of magnitude faster.

Our proposed feature builds on the well-known FAST keypoint detector [23] and the recently-developed BRIEF descriptor [6]; for this reason we call it ORB (Oriented

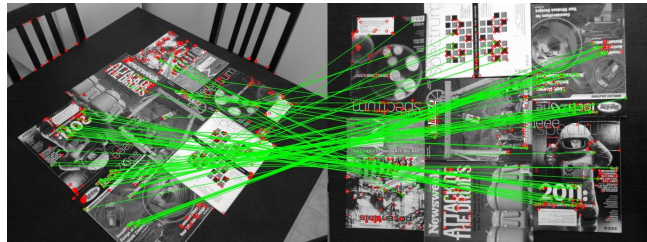


Figure 1. Typical matching result using ORB on real-world images with viewpoint change. Green lines are valid matches; red circles indicate unmatched points.

FAST and Rotated BRIEF). Both these techniques are attractive because of their good performance and low cost. In this paper, we address several limitations of these techniques vis-a-vis SIFT, most notably the lack of rotational invariance in BRIEF. Our main contributions are:

- The addition of a fast and accurate orientation component to FAST.
- The efficient computation of oriented BRIEF features.
- Analysis of variance and correlation of oriented BRIEF features.
- A learning method for de-correlating BRIEF features under rotational invariance, leading to better performance in nearest-neighbor applications.

To validate ORB, we perform experiments that test the properties of ORB relative to SIFT and SURF, for both raw matching ability, and performance in image-matching applications. We also illustrate the efficiency of ORB by implementing a patch-tracking application on a smart phone. An additional benefit of ORB is that it is free from the licensing restrictions of SIFT and SURF.

## 2. Related Work

**Keypoints** FAST and its variants [23, 24] are the method of choice for finding keypoints in real-time systems that match visual features, for example, Parallel Tracking and Mapping [13]. It is efficient and finds reasonable corner keypoints, although it must be augmented with pyramid

schemes for scale [14], and in our case, a Harris corner filter [11] to reject edges and provide a reasonable score.

Many keypoint detectors include an orientation operator (SIFT and SURF are two prominent examples), but FAST does not. There are various ways to describe the orientation of a keypoint; many of these involve histograms of gradient computations, for example in SIFT [17] and the approximation by block patterns in SURF [2]. These methods are either computationally demanding, or in the case of SURF, yield poor approximations. The reference paper by Rosin [22] gives an analysis of various ways of measuring orientation of corners, and we borrow from his centroid technique. Unlike the orientation operator in SIFT, which can have multiple value on a single keypoint, the centroid operator gives a single dominant result.

**Descriptors** BRIEF [6] is a recent feature descriptor that uses simple binary tests between pixels in a smoothed image patch. Its performance is similar to SIFT in many respects, including robustness to lighting, blur, and perspective distortion. However, it is very sensitive to in-plane rotation.

BRIEF grew out of research that uses binary tests to train a set of classification trees [4]. Once trained on a set of 500 or so typical keypoints, the trees can be used to return a signature for any arbitrary keypoint [5]. In a similar manner, we look for the tests least sensitive to orientation. The classic method for finding uncorrelated tests is Principal Component Analysis; for example, it has been shown that PCA for SIFT can help remove a large amount of redundant information [12]. However, the space of possible binary tests is too big to perform PCA and an exhaustive search is used instead.

Visual vocabulary methods [21, 27] use offline clustering to find exemplars that are uncorrelated and can be used in matching. These techniques might also be useful in finding uncorrelated binary tests.

The closest system to ORB is [3], which proposes a multi-scale Harris keypoint and oriented patch descriptor. This descriptor is used for image stitching, and shows good rotational and scale invariance. It is not as efficient to compute as our method, however.

### 3. oFAST: FAST Keypoint Orientation

FAST features are widely used because of their computational properties. However, FAST features do not have an orientation component. In this section we add an efficiently-computed orientation.

#### 3.1. FAST Detector

We start by detecting FAST points in the image. FAST takes one parameter, the intensity threshold between the center pixel and those in a circular ring about the center.

We use FAST-9 (circular radius of 9), which has good performance.

FAST does not produce a measure of cornerness, and we have found that it has large responses along edges. We employ a Harris corner measure [11] to order the FAST keypoints. For a target number  $N$  of keypoints, we first set the threshold low enough to get more than  $N$  keypoints, then order them according to the Harris measure, and pick the top  $N$  points.

FAST does not produce multi-scale features. We employ a scale pyramid of the image, and produce FAST features (filtered by Harris) at each level in the pyramid.

#### 3.2. Orientation by Intensity Centroid

Our approach uses a simple but effective measure of corner orientation, the *intensity centroid* [22]. The intensity centroid assumes that a corner’s intensity is offset from its center, and this vector may be used to impute an orientation. Rosin defines the moments of a patch as:

$$m_{pq} = \sum_{x,y} x^p y^q I(x,y), \quad (1)$$

and with these moments we may find the centroid:

$$C = \left( \frac{m_{10}}{m_{00}}, \frac{m_{01}}{m_{00}} \right) \quad (2)$$

We can construct a vector from the corner’s center,  $O$ , to the centroid,  $\vec{OC}$ . The orientation of the patch then simply is:

$$\theta = \text{atan2}(m_{01}, m_{10}), \quad (3)$$

where  $\text{atan2}$  is the quadrant-aware version of  $\arctan$ . Rosin mentions taking into account whether the corner is dark or light; however, for our purposes we may ignore this as the angle measures are consistent regardless of the corner type.

To improve the rotation invariance of this measure we make sure that moments are computed with  $x$  and  $y$  remaining within a circular region of radius  $r$ . We empirically choose  $r$  to be the patch size, so that that  $x$  and  $y$  run from  $[-r, r]$ . As  $|C|$  approaches 0, the measure becomes unstable; with FAST corners, we have found that this is rarely the case.

We compared the centroid method with two gradient-based measures, BIN and MAX. In both cases,  $X$  and  $Y$  gradients are calculated on a smoothed image. MAX chooses the largest gradient in the keypoint patch; BIN forms a histogram of gradient directions at 10 degree intervals, and picks the maximum bin. BIN is similar to the SIFT algorithm, although it picks only a single orientation. The variance of the orientation in a simulated dataset (in-plane rotation plus added noise) is shown in Figure 2. Neither of the gradient measures performs very well, while the centroid gives a uniformly good orientation, even under large image noise.

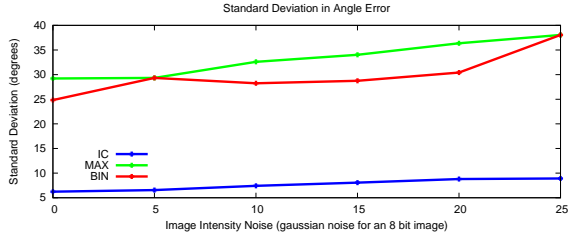


Figure 2. Rotation measure. The intensity centroid (IC) performs best on recovering the orientation of artificially rotated noisy patches, compared to a histogram (BIN) and MAX method.

## 4. rBRIEF: Rotation-Aware Brief

In this section, we first introduce a steered BRIEF descriptor, show how to compute it efficiently and demonstrate why it actually performs poorly with rotation. We then introduce a learning step to find less correlated binary tests leading to the better descriptor rBRIEF, for which we offer comparisons to SIFT and SURF.

### 4.1. Efficient Rotation of the BRIEF Operator

#### Brief overview of BRIEF

The BRIEF descriptor [6] is a bit string description of an image patch constructed from a set of binary intensity tests. Consider a smoothed image patch,  $\mathbf{p}$ . A binary test  $\tau$  is defined by:

$$\tau(\mathbf{p}; \mathbf{x}, \mathbf{y}) := \begin{cases} 1 & : \mathbf{p}(\mathbf{x}) < \mathbf{p}(\mathbf{y}) \\ 0 & : \mathbf{p}(\mathbf{x}) \geq \mathbf{p}(\mathbf{y}) \end{cases}, \quad (4)$$

where  $\mathbf{p}(\mathbf{x})$  is the intensity of  $\mathbf{p}$  at a point  $\mathbf{x}$ . The feature is defined as a vector of  $n$  binary tests:

$$f_n(\mathbf{p}) := \sum_{1 \leq i \leq n} 2^{i-1} \tau(\mathbf{p}; \mathbf{x}_i, \mathbf{y}_i) \quad (5)$$

Many different types of distributions of tests were considered in [6]; here we use one of the best performers, a Gaussian distribution around the center of the patch. We also choose a vector length  $n = 256$ .

It is important to smooth the image before performing the tests. In our implementation, smoothing is achieved using an integral image, where each test point is a  $5 \times 5$  sub-window of a  $31 \times 31$  pixel patch. These were chosen from our own experiments and the results in [6].

#### Steered BRIEF

We would like to allow BRIEF to be invariant to in-plane rotation. Matching performance of BRIEF falls off sharply for in-plane rotation of more than a few degrees (see Figure 7). Calonder [6] suggests computing a BRIEF descriptor for a set of rotations and perspective warps of each patch,

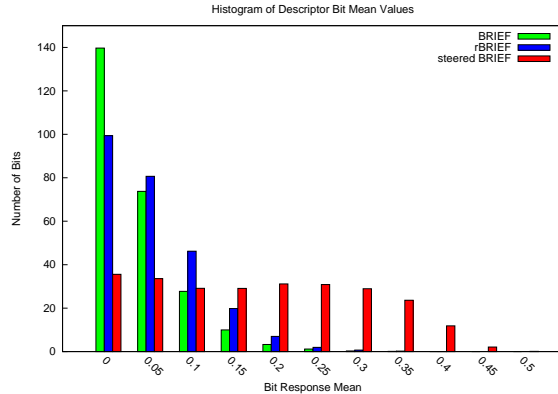


Figure 3. Distribution of means for feature vectors: BRIEF, steered BRIEF (Section 4.1), and rBRIEF (Section 4.3). The X axis is the distance to a mean of 0.5

but this solution is obviously expensive. A more efficient method is to steer BRIEF according to the orientation of keypoints. For any feature set of  $n$  binary tests at location  $(\mathbf{x}_i, \mathbf{y}_i)$ , define the  $2 \times n$  matrix

$$\mathbf{S} = \begin{pmatrix} \mathbf{x}_1, \dots, \mathbf{x}_n \\ \mathbf{y}_1, \dots, \mathbf{y}_n \end{pmatrix}$$

Using the patch orientation  $\theta$  and the corresponding rotation matrix  $\mathbf{R}_\theta$ , we construct a “steered” version  $\mathbf{S}_\theta$  of  $\mathbf{S}$ :

$$\mathbf{S}_\theta = \mathbf{R}_\theta \mathbf{S},$$

Now the steered BRIEF operator becomes

$$g_n(\mathbf{p}, \theta) := f_n(\mathbf{p}) | (\mathbf{x}_i, \mathbf{y}_i) \in \mathbf{S}_\theta \quad (6)$$

We discretize the angle to increments of  $2\pi/30$  (12 degrees), and construct a lookup table of precomputed BRIEF patterns. As long as the keypoint orientation  $\theta$  is consistent across views, the correct set of points  $\mathbf{S}_\theta$  will be used to compute its descriptor.

### 4.2. Variance and Correlation

One of the pleasing properties of BRIEF is that each bit feature has a large variance and a mean near 0.5. Figure 3 shows the spread of means for a typical Gaussian BRIEF pattern of 256 bits over 100k sample keypoints. A mean of 0.5 gives the maximum sample variance 0.25 for a bit feature. On the other hand, once BRIEF is oriented along the keypoint direction to give steered BRIEF, the means are shifted to a more distributed pattern (again, Figure 3). One way to understand this is that the oriented corner keypoints present a more uniform appearance to binary tests.

High variance makes a feature more discriminative, since it responds differentially to inputs. Another desirable property is to have the tests uncorrelated, since then each test will contribute to the result. To analyze the correlation and

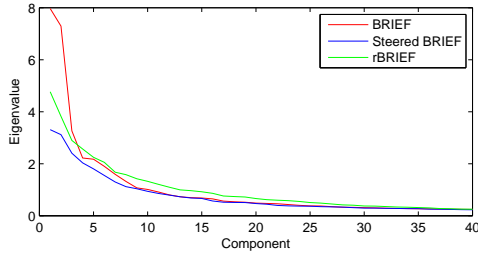


Figure 4. Distribution of eigenvalues in the PCA decomposition over 100k keypoints of three feature vectors: BRIEF (Section 4.1), and rBRIEF (Section 4.3).

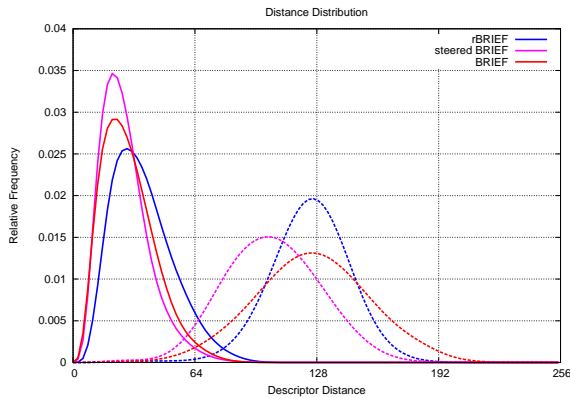


Figure 5. The dotted lines show the distances of a keypoint to outliers, while the solid lines denote the distances only between inlier matches for three feature vectors: BRIEF, steered BRIEF (Section 4.1), and rBRIEF (Section 4.3).

variance of tests in the BRIEF vector, we looked at the response to 100k keypoints for BRIEF and steered BRIEF. The results are shown in Figure 4. Using PCA on the data, we plot the highest 40 eigenvalues (after which the two descriptors converge). Both BRIEF and steered BRIEF exhibit high initial eigenvalues, indicating correlation among the binary tests – essentially all the information is contained in the first 10 or 15 components. Steered BRIEF has significantly lower variance, however, since the eigenvalues are lower, and thus is not as discriminative. Apparently BRIEF depends on random orientation of keypoints for good performance. Another view of the effect of steered BRIEF is shown in the distance distributions between inliers and outliers (Figure 5). Notice that for steered BRIEF, the mean for outliers is pushed left, and there is more of an overlap with the inliers.

### 4.3. Learning Good Binary Features

To recover from the loss of variance in steered BRIEF, and to reduce correlation among the binary tests, we develop a learning method for choosing a good subset of binary tests. One possible strategy is to use PCA or some other dimensionality-reduction method, and starting from a

large set of binary tests, identify 256 new features that have high variance and are uncorrelated over a large training set. However, since the new features are composed from a larger number of binary tests, they would be less efficient to compute than steered BRIEF. Instead, we search among all possible binary tests to find ones that both have high variance (and means close to 0.5), as well as being uncorrelated.

The method is as follows. We first set up a training set of some 300k keypoints, drawn from images in the PASCAL 2006 set [8]. We also enumerate all possible binary tests drawn from a  $31 \times 31$  pixel patch. Each test is a pair of  $5 \times 5$  sub-windows of the patch. If we note the width of our patch as  $w_p = 31$  and the width of the test sub-window as  $w_t = 5$ , then we have  $N = (w_p - w_t)^2$  possible sub-windows. We would like to select pairs of two from these, so we have  $\binom{N}{2}$  binary tests. We eliminate tests that overlap, so we end up with  $M = 205590$  possible tests. The algorithm is:

1. Run each test against all training patches.
2. Order the tests by their distance from a mean of 0.5, forming the vector T.
3. Greedy search:
  - (a) Put the first test into the result vector R and remove it from T.
  - (b) Take the next test from T, and compare it against all tests in R. If its absolute correlation is greater than a threshold, discard it; else add it to R.
  - (c) Repeat the previous step until there are 256 tests in R. If there are fewer than 256, raise the threshold and try again.

This algorithm is a greedy search for a set of uncorrelated tests with means near 0.5. The result is called rBRIEF. rBRIEF has significant improvement in the variance and correlation over steered BRIEF (see Figure 4). The eigenvalues of PCA are higher, and they fall off much less quickly. It is interesting to see the high-variance binary tests produced by the algorithm (Figure 6). There is a very pronounced vertical trend in the unlearned tests (left image), which are highly correlated; the learned tests show better diversity and lower correlation.

### 4.4. Evaluation

We evaluate the combination of oFAST and rBRIEF, which we call ORB, using two datasets: images with synthetic in-plane rotation and added Gaussian noise, and a real-world dataset of textured planar images captured from different viewpoints. For each reference image, we compute the oFAST keypoints and rBRIEF features, targeting 500 keypoints per image. For each test image (synthetic rotation or real-world viewpoint change), we do the same, then perform brute-force matching to find the best correspondence.



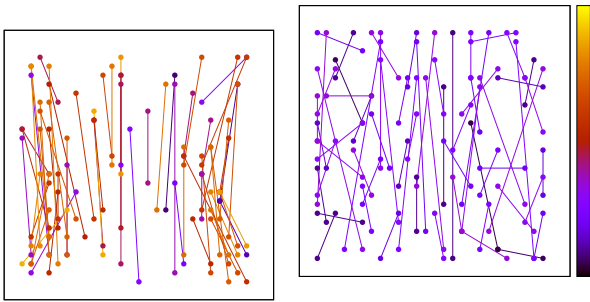


Figure 6. A subset of the binary tests generated by considering high-variance under orientation (left) and by running the learning algorithm to reduce correlation (right). Note the distribution of the tests around the axis of the keypoint orientation, which is pointing up. The color coding shows the maximum pairwise correlation of each test, with black and purple being the lowest. The learned tests clearly have a better distribution and lower correlation.

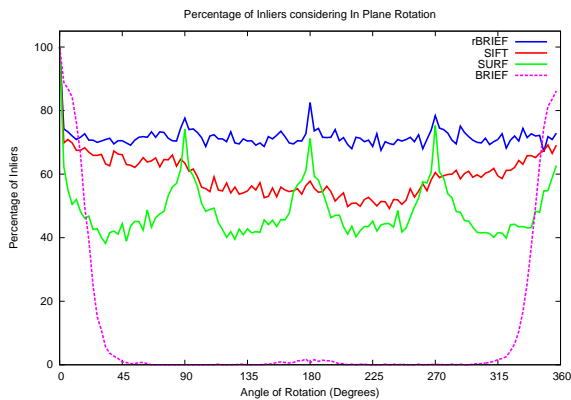


Figure 7. Matching performance of SIFT, SURF, BRIEF with FAST, and ORB (oFAST +rBRIEF) under synthetic rotations with Gaussian noise of 10.

The results are given in terms of the percentage of correct matches, against the angle of rotation.

Figure 7 shows the results for the synthetic test set with added Gaussian noise of 10. Note that the standard BRIEF operator falls off dramatically after about 10 degrees. SIFT outperforms SURF, which shows quantization effects at 45-degree angles due to its Haar-wavelet composition. ORB has the best performance, with over 70% inliers.

ORB is relatively immune to Gaussian image noise, unlike SIFT. If we plot the inlier performance vs. noise, SIFT exhibits a steady drop of 10% with each additional noise increment of 5. ORB also drops, but at a much lower rate (Figure 8).

To test ORB on real-world images, we took two sets of images, one our own indoor set of highly-textured magazines on a table (Figure 9), the other an outdoor scene. The datasets have scale, viewpoint, and lighting changes. Running a simple inlier/outlier test on this set of images,

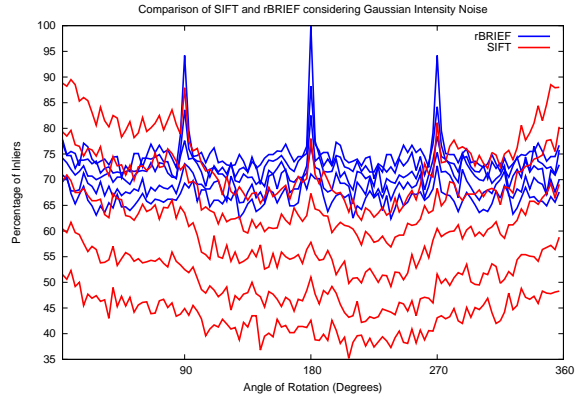


Figure 8. Matching behavior under noise for SIFT and rBRIEF. The noise levels are 0, 5, 10, 15, 20, and 25. SIFT performance degrades rapidly, while rBRIEF is relatively unaffected.

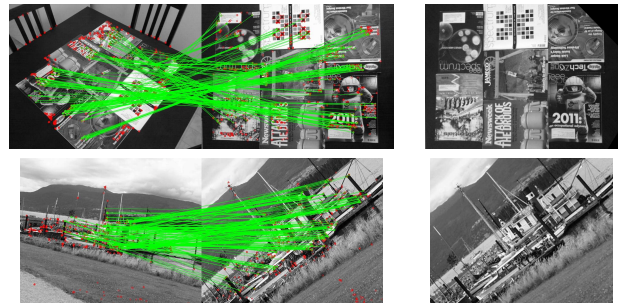


Figure 9. Real world data of a table full of magazines and an outdoor scene. The images in the first column are matched to those in the second. The last column is the resulting warp of the first onto the second.

we measure the performance of ORB relative to SIFT and SURF. The test is performed in the following manner:

1. Pick a reference view  $V_0$ .
2. For all  $V_i$ , find a homographic warp  $H_{i0}$  that maps  $V_i \rightarrow V_0$ .
3. Now, use the  $H_{i0}$  as ground truth for descriptor matches from SIFT, SURF, and ORB.

	inlier %	$N$ points
<b>Magazines</b>		
ORB	36.180	548.50
SURF	38.305	513.55
SIFT	34.010	584.15
<b>Boat</b>		
ORB	45.8	789
SURF	28.6	795
SIFT	30.2	714

ORB outperforms SIFT and SURF on the outdoor dataset. It is about the same on the indoor set; [6] noted that blob-detection keypoints like SIFT tend to be better on graffiti-type images.

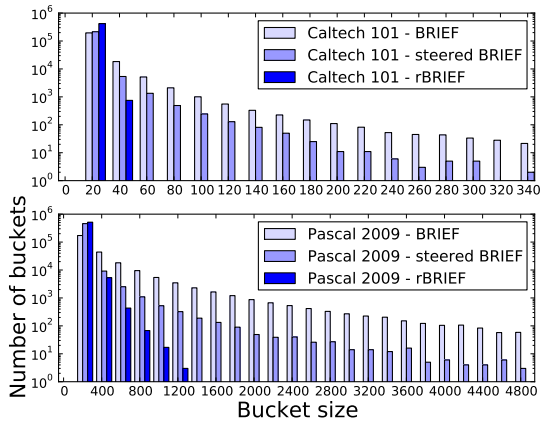


Figure 10. Two different datasets (7818 images from the PASCAL 2009 dataset [9] and 9144 low resolution images from the Caltech 101 [29]) are used to train LSH on the BRIEF, steered BRIEF and rBRIEF descriptors. The training takes less than 2 minutes and is limited by the disk IO. rBRIEF gives the most homogeneous buckets by far, thus improving the query speed and accuracy.

## 5. Scalable Matching of Binary Features

In this section we show that ORB outperforms SIFT/SURF in nearest-neighbor matching over large databases of images. A critical part of ORB is the recovery of variance, which makes NN search more efficient.

### 5.1. Locality Sensitive Hashing for rBrief

As rBRIEF is a binary pattern, we choose Locality Sensitive Hashing [10] as our nearest neighbor search. In LSH, points are stored in several hash tables and hashed in different buckets. Given a query descriptor, its matching buckets are retrieved and its elements compared using a brute force matching. The power of that technique lies in its ability to retrieve nearest neighbors with a high probability given enough hash tables.

For binary features, the hash function is simply a subset of the signature bits: the buckets in the hash tables contain descriptors with a common sub-signature. The distance is the Hamming distance.

We use multi-probe LSH [18] which improves on the traditional LSH by looking at neighboring buckets in which a query descriptor falls. While this could result in more matches to check, it actually allows for a lower number of tables (and thus less RAM usage) and a longer sub-signature and therefore smaller buckets.

### 5.2. Correlation and Leveling

rBRIEF improves the speed of LSH by making the buckets of the hash tables more even: as the bits are less correlated, the hash function does a better job at partitioning

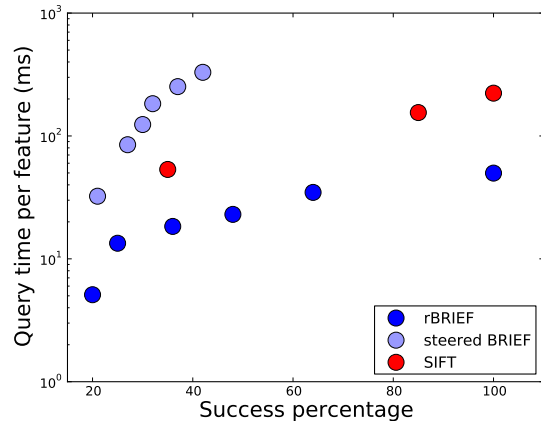


Figure 11. Speed vs. accuracy. The descriptors are tested on warped versions of the images they were trained on. We used 1, 2 and 3 kd-trees for SIFT (the autotuned FLANN kd-tree gave worse performance), 4 to 20 hash tables for rBRIEF and 16 to 40 tables for steered BRIEF (both with a sub-signature of 16 bits). Nearest neighbors were searched over 1.6M entries for SIFT and 1.8M entries for rBRIEF.

the data. As shown in Figure 10, buckets are much smaller in average compared to steered BRIEF or normal BRIEF.

### 5.3. Evaluation

We compare the performance of rBRIEF LSH with kd-trees of SIFT features using FLANN [20]. We train the different descriptors on the Pascal 2009 dataset and test them on sampled warped versions of those images using the same affine transforms as in [1].

Our multi-probe LSH uses bitsets to speedup the presence of keys in the hash maps. It also computes the Hamming distance between two descriptors using an SSE 4.2 optimized popcount.

Figure 11 establishes a correlation between the speed and the accuracy of kd-trees with SIFT (SURF is equivalent) and LSH with rBRIEF. A successful match of the test image occurs when more than 50 descriptors are found in the correct database image. We notice that LSH is faster than the kd-trees, most likely thanks to its simplicity and the speed of the distance computation. LSH also gives more flexibility with regard to accuracy, which can be interesting in bag-of-feature approaches [21, 27]. We can also notice that the steered BRIEF is much slower due to its uneven buckets.

## 6. Applications

### 6.1. Benchmarks

One emphasis for ORB is the efficiency of detection and description on standard CPUs. Our canonical ORB detector uses the oFAST detector and rBRIEF descriptor, each

computed separately on five scales of the image, with a scaling factor of  $\sqrt{2}$ . We used an area-based interpolation for efficient decimation.

The ORB system breaks down into the following times per typical frame of size 640x480. The code was executed in a single thread running on an Intel i7 2.8 GHz processor:

<b>ORB:</b>	Pyramid	oFAST	rBRIEF
Time (ms)	4.43	8.68	2.12

When computing ORB on a set of 2686 images at 5 scales, it was able to detect and compute over  $2 \times 10^6$  features in 42 seconds. Comparing to SIFT and SURF on the same data, for the same number of features (roughly 1000), and the same number of scales, we get the following times:

Detector	ORB	SURF	SIFT
Time per frame (ms)	<b>15.3</b>	217.3	5228.7

These times were averaged over 24 640x480 images from the Pascal dataset [9]. ORB is an order of magnitude faster than SURF, and over two orders faster than SIFT.

## 6.2. Textured object detection

We apply rBRIEF to object recognition by implementing a conventional object recognition pipeline similar to [19]: we first detect oFAST features and rBRIEF descriptors, match them to our database, and then perform PROSAC [7] and EPnP [16] to have a pose estimate.

Our database contains 49 household objects, each taken under 24 views with a 2D camera and a Kinect device from Microsoft. The testing data consists of 2D images of subsets of those same objects under different view points and occlusions. To have a match, we require that descriptors are matched but also that a pose can be computed. In the end, our pipeline retrieves 61% of the objects as shown in Figure 12.

The algorithm handles a database of 1.2M descriptors in 200MB and has timings comparable to what we showed earlier (14 ms for detection and 17ms for LSH matching in average). The pipeline could be sped up considerably by not matching all the query descriptors to the training data but our goal was only to show the feasibility of object detection with ORB.

## 6.3. Embedded real-time feature tracking

Tracking on the phone involves matching the live frames to a previously captured keyframe. Descriptors are stored with the keyframe, which is assumed to contain a planar surface that is well textured. We run ORB on each incoming frame, and proceed with a brute force descriptor matching against the keyframe. The putative matches from the descriptor distance are used in a PROSAC best fit homography  $H$ .

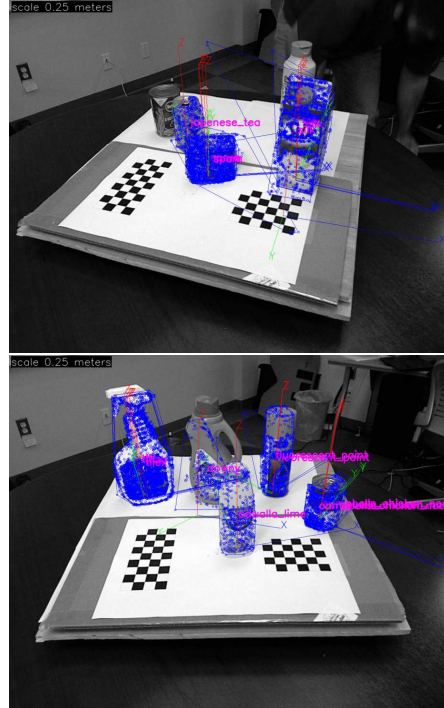


Figure 12. Two images of our textured object recognition with pose estimation. The blue features are the training features superimposed on the query image to indicate that the pose of the object was found properly. Axes are also displayed for each object as well as a pink label. Top image misses two objects; all are found in the bottom one.

While there are real-time feature trackers that can run on a cellphone [15], they usually operate on very small images (e.g., 120x160) and with very few features. Systems comparable to ours [30] typically take over 1 second per image. We were able to run ORB with  $640 \times 480$  resolution at 7 Hz on a cellphone with a 1GHz ARM chip and 512 MB of RAM. The OpenCV port for Android was used for the implementation. These are benchmarks for about 400 points per image:

	ORB	Matching	$H$ Fit
Time (ms)	66.6	72.8	20.9

## 7. Conclusion

In this paper, we have defined a new oriented descriptor, ORB, and demonstrated its performance and efficiency relative to other popular features. The investigation of variance under orientation was critical in constructing ORB and de-correlating its components, in order to get good performance in nearest-neighbor applications. We have also contributed a BSD licensed implementation of ORB to the community, via OpenCV 2.3.

One of the issues that we have not adequately addressed



here is scale invariance. Although we use a pyramid scheme for scale, we have not explored per keypoint scale from depth cues, tuning the number of octaves, etc.. Future work also includes GPU/SSE optimization, which could improve LSH by another order of magnitude.

## References

- [1] M. Aly, P. Welinder, M. Munich, and P. Perona. Scaling object recognition: Benchmark of current state of the art techniques. In *First IEEE Workshop on Emergent Issues in Large Amounts of Visual Data (WS-LAVD)*, *IEEE International Conference on Computer Vision (ICCV)*, September 2009. 6
- [2] H. Bay, T. Tuytelaars, and L. Van Gool. Surf: Speeded up robust features. In *European Conference on Computer Vision*, May 2006. 1, 2
- [3] M. Brown, S. Winder, and R. Szeliski. Multi-image matching using multi-scale oriented patches. In *Computer Vision and Pattern Recognition*, pages 510–517, 2005. 2
- [4] M. Calonder, V. Lepetit, and P. Fua. Keypoint signatures for fast learning and recognition. In *European Conference on Computer Vision*, 2008. 2
- [5] M. Calonder, V. Lepetit, K. Konolige, P. Mihelich, and P. Fua. High-speed keypoint description and matching using dense signatures. In *Under review*, 2009. 2
- [6] M. Calonder, V. Lepetit, C. Strecha, and P. Fua. Brief: Binary robust independent elementary features. In *In European Conference on Computer Vision*, 2010. 1, 2, 3, 5
- [7] O. Chum and J. Matas. Matching with PROSAC - progressive sample consensus. In C. Schmid, S. Soatto, and C. Tomasi, editors, *Proc. of Conference on Computer Vision and Pattern Recognition (CVPR)*, volume 1, pages 220–226, Los Alamitos, USA, June 2005. IEEE Computer Society. 7
- [8] M. Everingham. The PASCAL Visual Object Classes Challenge 2006 (VOC2006) Results. <http://pascallin.ecs.soton.ac.uk/challenges/VOC/databases.html>. 4
- [9] M. Everingham, L. Van Gool, C. K. I. Williams, J. Winn, and A. Zisserman. The PASCAL Visual Object Classes Challenge 2009 (VOC2009) Results. <http://www.pascal-network.org/challenges/VOC/voc2009/workshop/index.html>. 6, 7
- [10] A. Gionis, P. Indyk, and R. Motwani. Similarity search in high dimensions via hashing. In M. P. Atkinson, M. E. Orłowska, P. Valduriez, S. B. Zdonik, and M. L. Brodie, editors, *VLDB'99, Proceedings of 25th International Conference on Very Large Data Bases, September 7-10, 1999, Edinburgh, Scotland, UK*, pages 518–529. Morgan Kaufmann, 1999. 6
- [11] C. Harris and M. Stephens. A combined corner and edge detector. In *Alvey Vision Conference*, pages 147–151, 1988. 2
- [12] Y. Ke and R. Sukthankar. Pca-sift: A more distinctive representation for local image descriptors. In *Computer Vision and Pattern Recognition*, pages 506–513, 2004. 2
- [13] G. Klein and D. Murray. Parallel tracking and mapping for small AR workspaces. In *Proc. Sixth IEEE and ACM International Symposium on Mixed and Augmented Reality (ISMAR'07)*, Nara, Japan, November 2007. 1
- [14] G. Klein and D. Murray. Improving the agility of keyframe-based SLAM. In *European Conference on Computer Vision*, 2008. 2
- [15] G. Klein and D. Murray. Parallel tracking and mapping on a camera phone. In *Proc. Eighth IEEE and ACM International Symposium on Mixed and Augmented Reality (ISMAR'09)*, Orlando, October 2009. 7
- [16] V. Lepetit, F. Moreno-Noguer, and P. Fua. EPnP: An accurate O(n) solution to the pnp problem. *Int. J. Comput. Vision*, 81:155–166, February 2009. 7
- [17] D. G. Lowe. Distinctive image features from scale-invariant keypoints. *International Journal of Computer Vision*, 60(2):91–110, 2004. 1, 2
- [18] Q. Lv, W. Josephson, Z. Wang, M. Charikar, and K. Li. Multi-probe LSH: efficient indexing for high-dimensional similarity search. In *Proceedings of the 33rd international conference on Very large data bases, VLDB '07*, pages 950–961. VLDB Endowment, 2007. 6
- [19] M. Martinez, A. Collet, and S. S. Srinivasa. MOPED: A Scalable and low Latency Object Recognition and Pose Estimation System. In *IEEE International Conference on Robotics and Automation*. IEEE, 2010. 7
- [20] M. Muja and D. G. Lowe. Fast approximate nearest neighbors with automatic algorithm configuration. *VISAPP*, 2009. 6
- [21] D. Nistér and H. Stewénius. Scalable recognition with a vocabulary tree. In *CVPR*, 2006. 2, 6
- [22] P. L. Rosin. Measuring corner properties. *Computer Vision and Image Understanding*, 73(2):291 – 307, 1999. 2
- [23] E. Rosten and T. Drummond. Machine learning for high-speed corner detection. In *European Conference on Computer Vision*, volume 1, 2006. 1
- [24] E. Rosten, R. Porter, and T. Drummond. Faster and better: A machine learning approach to corner detection. *IEEE Trans. Pattern Analysis and Machine Intelligence*, 32:105–119, 2010. 1
- [25] S. Se, D. Lowe, and J. Little. Mobile robot localization and mapping with uncertainty using scale-invariant visual landmarks. *International Journal of Robotic Research*, 21:735–758, August 2002. 1
- [26] S. N. Sinha, J. Michael Frahm, M. Pollefeys, and Y. Genc. Gpu-based video feature tracking and matching. Technical report, In *Workshop on Edge Computing Using New Commodity Architectures*, 2006. 1
- [27] J. Sivic and A. Zisserman. Video google: A text retrieval approach to object matching in videos. *International Conference on Computer Vision*, page 1470, 2003. 2, 6
- [28] N. Snavely, S. M. Seitz, and R. Szeliski. Skeletal sets for efficient structure from motion. In *Proc. Computer Vision and Pattern Recognition*, 2008. 1
- [29] G. Wang, Y. Zhang, and L. Fei-Fei. Using dependent regions for object categorization in a generative framework, 2006. 6
- [30] A. Weimert, X. Tan, and X. Yang. Natural feature detection on mobile phones with 3D FAST. *Int. J. of Virtual Reality*, 9:29–34, 2010. 7